Journal of Applied Research and Technology

www.jart.icat.unam.mx

Journal of Applied Research and Technology 23 (2025) 362-370

Original

Assessing the effect of $LiClO_4$ electrolyte on the electrochemical properties of indium tin oxide thin films

I. Perez[a]* • V. Sosa[b] • F. Gamboa[b] • J. L. Enriquez-Carrejo[c] • J. C. Mixteco-Sanchez[d]

[a]*Consejo Nacional de Humanidades, Ciencias y Tecnologías (CONAHCYT)-Departamento de Física y Matemáticas, Instituto de Ingeniería y Tecnología, Universidad Autónoma de Ciudad Juárez, Juárez, Chihuahua, México*
[b]*Departamento de Física Aplicada, CINVESTAV Unidad Mérida, Mérida, Yucatán, México*
[c]*Departamento de Física y Matemáticas, Instituto de Ingeniería y Tecnología, Universidad Autónoma de Ciudad Juárez, Juárez, Chihuahua, México*
[d]*Departamento de Ciencias Naturales y Exactas, CU Valles, Universidad de Guadalajara, Jalisco, México*

Received 07 09 2024; accepted 10 02 2024
Available 08 31 2025

Abstract: In this research, we used a combination of experimental techniques to shed some light on the effect of lithium perchlorate ($LiClO_4$) on the electrochemical and physical properties of indium tin oxide (ITO) films. For this, we studied the effect of ITO films immersed in a $LiClO_4$/PC+EC solution. Chronoamperometry, along with transmissivity measurements, shows that ITO undergoes optical changes as a function of voltage changes. However, as the number of cycles increases, the transmissivity decreases significantly due to ITO degradation. Cyclic voltammetry reveals the presence of reduction and oxidation processes, suggesting ITO reduction and possible ion trapping. X-ray diffraction does not show compelling signs of lithium insertion or the presence of other phases. Finally, X-ray photoelectron spectroscopy is used to evaluate the oxidation states and chemical bonding. The analysis reveals the presence of indium oxide, suggesting that the surface is mainly ITO, in agreement with XRD studies.

Keywords: Electrochemical, reduction, degradation.

*Corresponding author.
E-mail address: israel.perez@uacj.mx (I. Perez).
Peer Review under the responsibility of Universidad Nacional Autónoma de México.

1. Introduction

Indium tin oxide (ITO) is the most common transparent conductive oxide (TCO) used today (Akanda et al., 2020; Minami, 2008). It possesses remarkable optical and transport properties, with a transmissivity higher than 80% and an excellent resistivity of less than 10^-4 Ω cm. Its applications range from displays to solar cells, touchscreens, electrochromic devices (ECDs), and electrochromic batteries (Wu et al., 2018). The conductivity and optical properties heavily depend on the operating conditions of the devices. Many of these devices use a thin layer of ITO that interacts with several other materials. Of importance for electrochromic applications, it is thought that ITO may interact with Li-based solutions comprising the electrolytes in ECDs and multifunctional devices.

The effect of Li insertion/extraction in ITO thin films has been considered by several researchers in the past (Bressers & Meulenkamp, 1998; Cogan et al., 1985; Corradini et al., 1990; Goldner et al., 1985; Macher et al., 2020; Svensson & Granqvist, 1985). Although some findings are contradictory, most likely due to different fabrication conditions, there is no doubt that ion insertion has strong effects on the optical and transport properties of ITO. For instance, Liu et al. have induced ITO reduction by electrochemical insertion of several anions (SO_4^{2-}, Cl^-, Br^-, SO_3^-) showing that the nonlinear optical properties can be manipulated as a function of the reduction agent (Liu et al., 2015). In another work, reduction of ITO was induced by exposing commercial ITO thin films to a SiO_2 solution (Folcher et al., 1997). This study reported a great change in the electrical resistance and variations in coloration from transparent to dark and gray.

Aware that the electrical and optical properties of ITO strongly depend on the electrolytic media (Folcher et al., 1997; Spada et al., 2013), in this work, we report on the effect of $LiClO_4$ electrolyte on the chemical, electrochemical, structural, and optical characteristics of commercial ITO films. Our purpose is to identify the possible role played by Li^+ cations on the electrochemical properties of ITO thin films. Recently, this idea has been explored in fluorine-doped tin oxide (FTO)-based ECDs (Perez, 2023; Wang et al., 2019). Nonetheless, FTO is not the most common TCO used in such devices, and we thus feel that a deeper investigation into ITO films is valuable. This research might be of particular interest to the electronic industry and researchers working with ECDs and multifunctional devices.

To reach this goal, we have used a variety of experimental techniques, including scanning electron microscopy (SEM), X-ray diffraction (XRD), cyclic voltammetry (CV), transmissivity along with chronoamperometry (CA), and X-ray photoelectron spectroscopy (XPS) of the In 3d, Sn 3d, O 1s, and Li 1s core levels. With these tools, we investigate the effect of lithium perchlorate solution on the morphology as well as on the crystalline, electrochemical, and chemical properties of commercial ITO samples.

2. Materials and methods

2.1. Experimental

We used two ITO/glass thin films acquired from MTI corporation, Richmond, CA, USA. The area of the samples is 2.5 cm×2.5 cm. The thickness of the glass and the ITO film is 0.7 mm and 180 nm, respectively. According to the manufacturer, the sheet resistance of the films ranges from 8 to 10 Ω/sq. ITO samples contain In_2O_3 and SnO_2 in 90 at% and 10 at%, respectively. One of the samples was dipped into the electrochemical solution, as described in Subsection 2.2, while the other was kept as a reference. The former is, henceforth, called LiITO, and the latter the as-received (ITO-AR) sample.

2.2. Characterization

Electrochemical properties are studied by cyclic voltammetry and chronoamperometry, using a CorrTest CS350 electrochemical workstation. For the CV measurements, a scan rate of 0.05 V/s in the potential interval from -2 V to +2 V for 30 cycles was used. To assess possible degradation, we carried out CA measurements for 100 cycles with steps of 10 s. A typical three-electrode setup is adopted for both measurements. Platinum and $Ag/AgCl_{KCl}$ electrodes play the role of counter and reference electrodes, respectively. The sample is used as a working electrode, and the three electrodes are placed in a cubic optoelectrochemical cell filled with the Li-based solution under dry conditions. The electrolytic solution amounts to 110 cm^3 of 1 M $LiClO_4$ dissolved in PC and EC. To remove any residues of water and avoid contamination, the lithium salts were preheated at 140 °C for 1 h and the solution was prepared in a glove box under argon atmosphere (water content < 8 ppm).

For the assessment of optical properties of ITO, transmissivity during CA measurements is acquired at a fixed wavelength of 637 nm, using a high-sensitivity sensor, Pasco (model CI-6604), connected to a Pasco interface UI-500.

Surface morphology before and after lithium exposure of the samples is studied by SEM with a field emission microscope JSM7000F. The possible effect of lithium insertion on the atomic structure is evaluated by XRD using a Siemens diffractometer model D-5000 with Cu K_α radiation (λ =1.5406 Å). XRD patterns were measured at steps of 0.0016° with a time per step of 3 s in a Bragg-Bretano configuration.

To assess the chemical properties of the samples, the In 3d, Sn 3d, O 1s, and Li 1s core levels were measured with a Thermo Scientific K-Alpha XPS spectrometer. Details of the parameters used can be found elsewhere (Perez et al., 2018; Perez et al., 2019, Perez et al., 2021). Oxidation states and atomic bonding

are determined by fitting the experimental data using a Tougaard background and Voigt functions as implemented in the CasaXPS software (version 2.3.19PR1.0). In and Sn spectra are deconvoluted using doublets with spin-orbit splittings of 7.51 eV and 8.42 eV, respectively. Table 1 shows a summary of the characterization conditions for the two samples.

Table 1. Characterization conditions for the samples. SEI=secondary electron imaging, COMPO=composition, TOPO=topography, SR=Scan rate, PW=Potential window, NC=number of cycles, CL=Core Levels, ST=step time, DST=degree step per time, λ =wavelength of light.

Technique-sample	ITO-AR	LiITO
SEM	15 kV: SEI, COMPO, TOPO	15 kV: SEI, COMPO, TOPO
XRD	Bragg-Bretano, DST=0.0016°/3 s, λ=1.5406 Å	Bragg-Betano, DST=0.0016°/3 s, λ=1.5406 Å
CV	---	SR=0.05 V/s, PW= ±2 V, NC=30
CA	---	ST=10 s, PW=± 2 V, NC=100
Transmissivity	---	λ =637 nm
XPS	CL=C 1s, In 3d, Sn 3d, O 2p	CL=C 1s, In 3d, Sn 3d, O 2p, Li 1s

3. Results and discussion

3.1. Electrochemical and optical properties

To define a safe potential interval for the CV and CA measurements, we first performed preliminary tests. During these experiments, we observed that for potentials less than -3 V, the samples turned blackish (not shown). Bressers and Meulenkamp (1998) also reported observing a metallic black color in films with ITO reduction below -2 V, which was interpreted as a sign of ITO degradation. We thus set an electroactive window from -2 V to 2 V.

CV measurements were carried out to study the electrochemical characteristics. The results are depicted in Fig. 1(a). As a reference, the ITO-AR sample looked transparent to the naked eye. During these measurements, the sample's color changed from transparent to yellowish from positive to negative potentials (cathodic potential), this change might be induced by Li transport from the electrolyte into the film. Indeed, this coloration was reported by other authors (Bressers & Meulenkamp, 1998; Cogan et al., 1985) and was interpreted as Li intercalation. The sample returns to its initial state in the reverse order, transporting Li^+ ions from the film.

At about -0.9 V, we observe an oxidation peak at anodic potentials (from negative to positive potentials) that can be associated with the oxidation of metallic In. Bressers and Meulenkamp (1998) also observed this behavior and interpreted it as Li intercalation. However, the presence of a strong reduction peak at -1.7 V reveals a severe ITO reduction. This agrees with the findings of Macher et al., who reported a reduction peak on ITO/PET samples using an electrolyte of LiTFSI/PC (Macher et al., 2020). This behavior can be the cause of degradation in ECDs (Wen et al, 2015). We also point out that the intensity of the oxidation peak increases as a function of cycle number (the arrow in the graph represents the direction of increase from cycle 1 all the way to cycle 100), which can also be associated with ITO reduction.

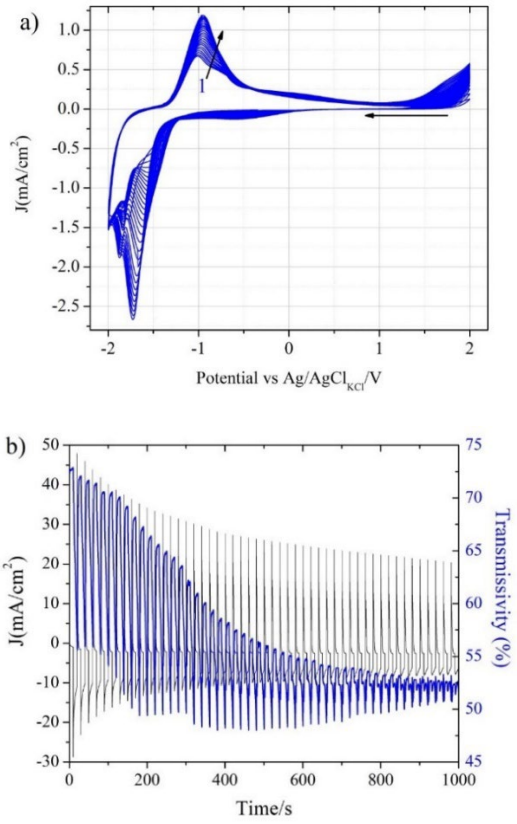

Figure 1. (a) Voltammograms; (b) Transmissivity (blue) along with chronoamperometry measurements (black). The number "1" in the CV graph indicates the first cycle, and the adjacent arrow indicates the direction of the cycle increment. The arrow on the right indicates the direction of the cycle.

The transmissivity of the samples, along with CA measurements, is displayed in Fig. 1 (b). We observe that a yellowish coloration appears for negative currents (or equivalently, negative voltages). The transmissivity for both cases decreases as the number of cycles increases, reaching a minimum, and then undergoing severe suppression after 40 cycles, suggesting possible degradation. Starting from the first

cycle, the transmissivity for the initial state (T_b) at λ = 637 nm is about 73.1% with a value for the colored state (T_c) of 56%. For the last cycle, the values are 53% and 50.5%, respectively. Considering possible electrochromism of the sample, the coloration efficiency η is defined as

$$\eta = \frac{ln\left(\frac{T_b}{T_c}\right)}{Q_x} \quad (1)$$

where Q_x is the extracted/inserted charge. This can be obtained from CA data by integration under the curve as a function of time. Accordingly, it is found that the charge inserted (Q_{in}) for the first cycle is 68 mC and the charge extracted (Q_x) is 28 mC. This yields a reversibility for the first cycle of K_1=Q_{in}/Q_{out}=0.41. Similarly, for the last cycle the inserted (extracted) charge is 43 mC (10 mC), so the reversibility for the 100th cycle is K_{100}=0.23. The corresponding coloration efficiencies are, respectively, 9.5 cm^2/C and 4.8 cm^2/C. These values are relatively low for practical applications if compared to those of the most common electrochromic materials, NiO (50 cm^2/C @ 550 nm) and WO^3 (54.8 cm^2/C @ 633 nm) (Acuña et al., 2021; Mahmoudi et al. 2016). At the end of the 100 cycles, the sample color became brownish, and reversibility is no longer possible. The overall behavior suggests electrochemical degradation, thus reducing the efficiency as the number of cycles increases. This seems to be accompanied by some degree of ITO reduction.

3.2. Morphology and effect of lithium on crystalline structure

Figure 2 presents the observations from SEM. The first micrograph shows the ITO-AR sample, which exhibits the typical flake-like morphology of ITO (Liu et al., 2015). This morphology is common in samples with high conductivity. After the electrochemical tests, the LiITO sample was left in a colored state, cleaned with ethylene carbonate and taken to the microscope. We observe that the sample forms an inhomogeneous layer with black zones (Fig. 2b). These zones are believed to be dissolution zones attacked by the electrolyte, leading to changes in the total transmissivity. Secondary electron images and topographic images also confirm this view (Fig. 2c and 2d). We also observe small grains with diameters ranging from a few nanometers to about 100 nm, which are distributed all over the surface. They are clearly from a different composition from the rest of the sample. An EDS analysis carried out on single grains showed a slight increase (about 3%) in In at%, suggesting that the grains are formed by metallic indium, possibly derived from ITO reduction. Spherical particles of metallic indium have been reported before (Liu et al., 2015; Spada et al., 2013) in which ITO was electrochemically treated with several electrolytes. The formation of grains was attributed to ITO reduction. Although the morphology in our sample differs from previous reports, we do not rule out the possibility that the same mechanism causes it. However, the differences can be attributed to the use of different electrolytes.

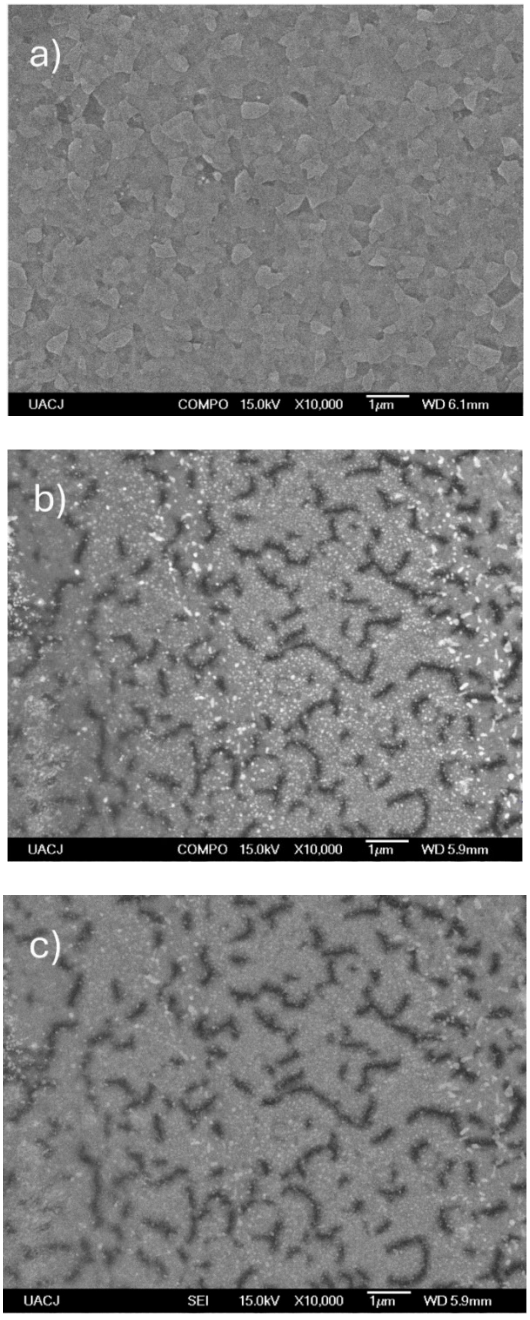

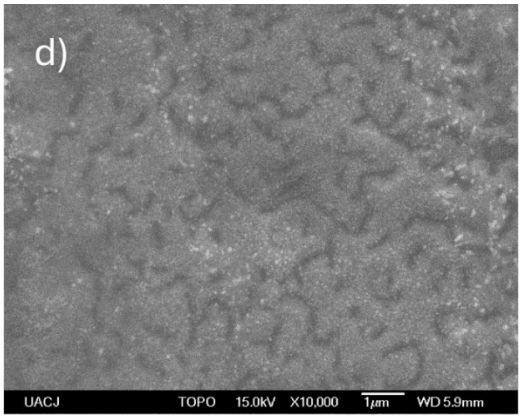

Figure 2. a) ITO AR. b)-d) Electrochemically treated sample with different electron modes. Some grains are observed on top of the sample indicating degradation. b) Compositional image, c) Secondary electron image, and d) topographic image.

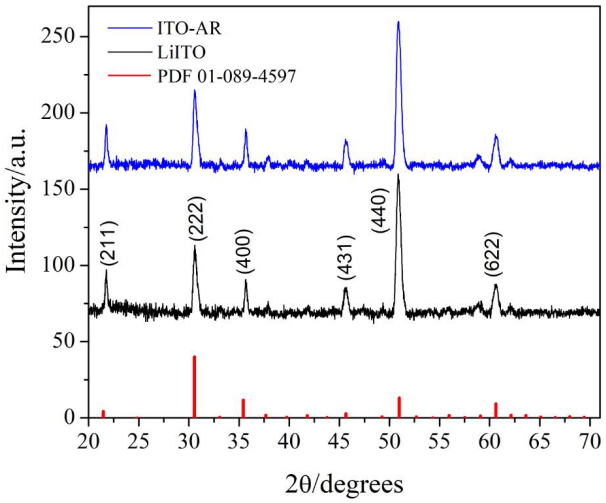

Figure 3. XRD for ITO-AR (blue spectrum) and LiITO (black spectrum) as compared to ITO reference PDF 01-089-4597 (red vertical lines). No peak displacement is observed.

The lattice of In_2O_3 has a body-centered-cubic structure belonging to space group Ia-3 (No. 206). The experimental lattice parameter is a=10.1170 Å, and the unit cell contains 8 formula units for a total of 40 atoms per unit cell. ITO is formed by replacing one In atom in the 40-atom cell with a Sn atom at the 8b sites, which corresponds to a 6.25 at% Sn doping. It is well known that if ion intercalation takes place, ions enter as interstitial defects and one should be able to observe changes in the crystalline structure (Ingham et al., 2005; Perez et al., 2021). A large number of impurities drive the material into phase transitions, while small amounts can induce variations in the lattice parameters that might be observed with X-ray diffraction (Ingham et al., 2005; Monk et al., 2007; Zhong et al., 1992; Pramudita et al., 2017). According to our own density functional theory calculations of Li-doped ITO, Li insertion of 2.5% in the supercell of ITO would induce an increase in the unit volume of about 5%. Figure 3 displays the results from XRD of both samples compared to the main phase of ITO ($In_{1.875}Sn_{0.125}O_3$) and taken as reference from crystallographic data files (PDF 01-089-4597). We observed six prominent peaks located at (21.7, 30.7, 35.7, 45.5, 51.1, 60.8)° that compare well with the reference (red vertical solid lines). Both of our samples exhibit a preferential orientation in the [440] direction. By comparing the diffractograms of both samples, no peak displacement is spotted, indicating a stable structure and no changes in cell parameters. It has been argued (Bressers & Meulenkamp, 1998) that charge insertion equal or greater than 5 mC/cm^2, corresponding to a stoichiometry of $Li_{0.1}ITO$, would induce a remarkable change in cell structure. However, our findings suggest that if there is a charge insertion, it is pretty low to be detected by XRD. It is worth mentioning that we do not observe traces of additional phases such as metallic In or $In(OH)_3$ whose main peaks should have appeared at 33.1 °C and 22.3 °C, respectively (Smith & Schneider, 1964; Mullica et al., 1979). These findings indicate that the only phase present corresponds to ITO.

3.3. Bonding and oxidation states

The chemical properties of both samples were determined by XPS analysis. Again, the XPS analysis for the LiITO sample was carried out after applying -2 V. Figure 4 shows the XPS spectrum for the C 1s, In 3d, Sn 3d, and O 1s core levels. The carbon core level was taken, on one hand, to determine the level of contamination and, on the other, to establish a core level standard. The data were fitted with three Gaussian line shapes [see Fig. 4(a) and (b)], whose main peaks are located at 284.7 eV, 286.0 eV, and 288.2 eV. The peaks are attributed to graphitic carbon, carbon dioxide (CO_2), and to carboxyl groups, respectively. This kind of contamination is typically found on air-exposed surfaces (Moulder et al., 1992; Shiratsuchi et al, 1992; Kuo, 1992; Pollard & Puddephatt, 1999).

The XPS signal for In and Sn 3d core levels is resolved each into two doublets with $3d_{5/2}$ and $3d_{3/2}$ suborbitals caused by spin-orbit interaction; these are separated by 7.50 eV and 8.42 eV, respectively [see Fig. 4 (c)-(f)]. The ITO-AR sample shows the In $3d_{5/2}$ peaks at positions 444.1 eV and 445.2 eV in agreement with the literature (Liu et al., 2015; Moulder et al., 1992; Fan & Goodenough, 1977). The first one is attributed to In-O bond in the In^{3+} valence state as part of In_2O_3, while the other peak has been attributed to indium suboxides (InO_x). No traces of metallic indium are spotted. Similarly, we observe two doublets with the Sn $3d_{5/2}$ peaks at 486.2 eV and 487.2 eV. The high-energy feature corresponds to the Sn-O bond in the Sn4+ oxidation state, forming SnO_2. The second one belongs to tin suboxides (SnO_x), most probably SnO (Fan & Goodenough, 1977; Grust et al., 1973), and again no traces of Sn reduction are spotted. For the lithiated sample [see Fig. 4(d) and (f)], there is no change in the peak positions for In 3d core line. The absence of the energy shift indicates that the oxidation state for In remains unaffected.

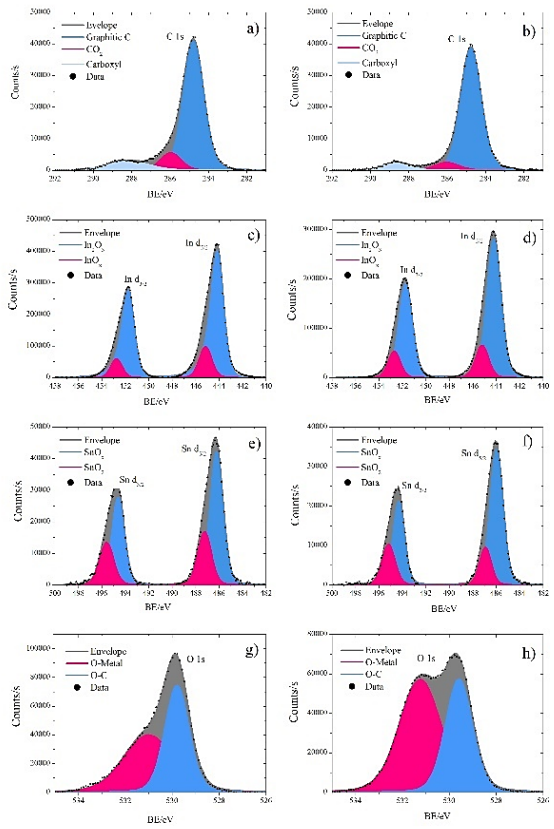

Figure 4. XPS spectra for C 1s (a and b), In 3d (c and d), Sn 3d (e and f) and O 1s (g and h) core levels. Left column for as-received ITO and right one for LiITO. See text for discussion.

Fig. 4(g) shows the O 1s core level for the ITO-AR sample. This signal was deconvoluted into two main Gaussian peaks located at 529.8 eV (blue peak) and 531.0 eV (pink peak). These two signals also appear for the LiITO sample [see Fig. 4(h)], but they are slightly shifted 0.1 eV to lower energies. The low energy peak is due to O-metal bond in O^{2-} oxidation state. The higher one is due to carbon contamination, as discussed above (Perez et al., 2018; Perez et al., 2019; Pollard & Puddephatt, 1999; Ke et al., 2015; Ren et al., 2018). In LiITO, we can see that the low-energy peak has a much higher intensity than in ITO-AR. Since this sample was dipped into the electrolytic solution, we think that some amount of lithium hydroxide (LiOH) was produced and remained on the surface after the electrochemical tests. LiOH could have been formed during sample handling or electrochemical measurements, as environmental water is challenging to eliminate, even under controlled conditions. Evidence for the generation of metal hydroxides in samples dipped in $LiClO_4$ solutions has been reported earlier (Acuña et al., 2021). To check this issue, we also measured the Li 1s core level of the LiITO sample [see Fig. 5]. The signal was deconvoluted into two mainly Gaussian peaks located at 55.0 eV and 55.5 eV. The first binding energy peak is due to the presence of LiOH (Dupin et al, 2000). The significant contribution to the whole signal comes from this peak. The second minor peak is attributed to Li-O bonding that corresponds to Li_2O present in the sample in low quantities.

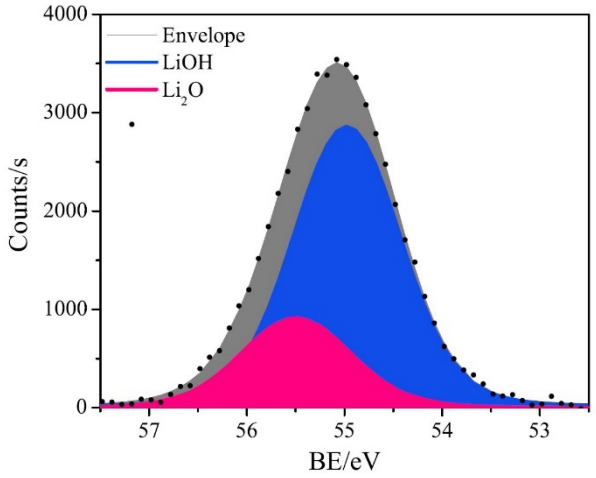

Figure 5. XPS spectra for Li 1s of LiITO.

4. Summary and conclusions

By using a series of experimental techniques, we have investigated the effect of $LiClO_4$ electrolyte on the electrochemical, structural, and morphological properties of commercial ITO films. Electrochemical measurements show that the chemical solution affects the transmittance due to a change in coloration at negative voltages. As the number of cycles increases, the transmissivity is significantly suppressed; we believe this could be due to possible sample degradation as evidenced by chronoamperometry tests combined with transmissivity. SEM images seem to support such a scenario, indicated by the presence of a layer with dark zones, where it is thought that the electrolyte attacks the surface film. On the other hand, XRD studies did not reveal changes in the lattice parameters of the LiITO sample, suggesting that Li does not go deep into the lattice. However, we do not rule out an accumulation on the surface. XPS verified this assumption. The analysis of the Sn 3d, In 3d, O 1s, and Li 1s core levels did not show a noticeable effect on the oxidation states. Still, we observe the presence of Li on the surface, confirming our assumption that lithium resides on a thin layer atop. These results could support researchers and technologists working on the development of ECDs, smart windows, touchscreens, multifunctional devices such as electrochromic batteries, and other devices where ITO is used in combination with lithium-based solutions with an emphasis on lithium perchlorate.

Lastly, it is worth mentioning that the research conducted here does not address an important question regarding the

dynamics of ions in the electrolyte and in the ITO surface. As is well known, mass transport can manifest via three modes: convection, migration, and diffusion. If no mechanical forces act on the solution, one can rule out the first mode. On the other hand, migration and diffusion can manifest even in the absence of mechanical forces and are more complex mechanisms that require deeper studies. Characterization techniques, including voltammetry in combination with electrochemical impedance spectroscopy (EIS), could be key to answering this question. Voltammetry carried out at different scan rates can give information on the diffusion coefficient of the oxidized analyte using the Randles-Sevcik equation. According to this equation, there is a linear dependence between the peak current (I_p) and the square root of the scan rate ($\sqrt{\nu}$) that can reveal diffusion mechanisms involved. On the other hand, EIS can shed some light on the resistance associated with charge transfer at the electrode-electrolyte interface. This provides insight into the kinetics of the electrochemical reactions occurring at the ITO surface. EIS can give clues as to how the analyte interacts with the electrode, including binding characteristics or competitive reactions. Also, EIS can reveal diffusion-related processes, especially if there is a Warburg impedance element in the Nyquist plot. This can indicate the diffusion of the analyte to the electrode surface and can provide information about mass transport limitations. These investigations go beyond the scope of the present paper and will be addressed in a future contribution.

CRediT authorship contribution statement

Israel Perez conceived the project, obtained the funding, carried out the electrochemical tests, obtained XRD and SEM data, analyzed the data, and wrote the manuscript. Victor Sosa and Fidel Gamboa performed the XPS and optical measurements and analyzed the data. Jose Enriquez obtained the funding and analyzed the data. Juan Mixteco analyzed the data. All the authors reviewed, discussed, and commented on the manuscript.

Conflict of interest

The authors do not have any conflict of interest to declare.

Acknowledgements

The authors gratefully acknowledge the support from the Consejo Nacional de Humanidades, Ciencias y Tecnologías (CONAHCYT), Mexico under project 3035. Special thanks to William Cauich for technical support during the XPS sessions.

Funding

The authors received no specific funding for this work.

References

Acuña, J. R. A., Perez, I., Sosa, V., Gamboa, F., Elizalde, J. T., Farías, R., ... & Mani, P. (2021). Sputtering power effects on the electrochromic properties of NiO films. *Optik*, *231*, 166509. https://doi.org/10.1016/j.ijleo.2021.166509

Akanda, M. R., Osman, A. M., Nazal, M. K., & Aziz, M. A. (2020). Recent advancements in the utilization of indium tin oxide (ITO) in electroanalysis without surface modification. *Journal of The Electrochemical Society*, *167*(3), 037534. https://doi.org/10.1149/1945-7111/ab64bd

Bressers, P. M., & Meulenkamp, E. A. (1998). The electrochromic behavior of indium tin oxide in propylene carbonate solutions. *Journal of the electrochemical society*, *145*(7), 2225. https://doi.org/10.1149/1.1838624

Cogan, S. F., Anderson, E. J., Plante, T. D., & Rauh, R. D. (1985). Electrochemical investigation of electrochromism in transparent conductive oxides. *Applied optics*, *24*(15), 2282-2283. https://doi.org/10.1364/AO.24.002282

Corradini, A., Marinangeli, A. M., & Mastragostino, M. (1990). Ito as counter-electrode in a polymer based electrochromic device. *Electrochimica Acta*, *35*(11-12), 1757-1760. https://doi.org/10.1016/0013-4686(90)87076-E

Dupin, J. C., Gonbeau, D., Vinatier, P., & Levasseur, A. (2000). Systematic XPS studies of metal oxides, hydroxides and peroxides. *Physical Chemistry Chemical Physics*, *2*(6), 1319-1324. https://doi.org/10.1039/A908800H

Fan, J. C., & Goodenough, J. B. (1977). X-ray photoemission spectroscopy studies of Sn-doped indium-oxide films. *Journal of applied physics*, *48*(8), 3524-3531. https://doi.org/10.1063/1.324149

Folcher, G., Cachet, H., Froment, M., & Bruneaux, J. (1997). Anodic corrosion of indium tin oxide films induced by the electrochemical oxidation of chlorides. *Thin Solid Films*, *301*(1-2), 242-248. https://doi.org/10.1016/S0040-6090(97)00024-2

Goldner, R. B., Foley, G., Goldner, E. L., Norton, P., Wong, K., Haas, T., ... & Chapman, R. (1985). Electrochromic behavior in ITO and related oxides. *Applied optics*, *24*(15), 2283-2284.

Grutsch, P. A., Zeller, M. V., & Fehlner, T. P. (1973). Photoelectron spectroscopy of tin compounds. *Inorganic Chemistry*, *12*(6), 1431-1433. https://doi.org/10.1021/ic50124a045

Ingham, B., Hendy, S. C., Chong, S. V., & Tallon, J. L. (2005). Density-functional studies of tungsten trioxide, tungsten bronzes, and related systems. *Physical Review B—Condensed Matter and Materials Physics*, *72*(7), 075109. https://doi.org/10.1103/PhysRevB.72.075109

Ke, W., Fang, G., Liu, Q., Xiong, L., Qin, P., Tao, H., & Yan, Y. (2015). Low-temperature solution-processed tin oxide as an alternative electron transporting layer for efficient perovskite solar cells. *Journal of the American Chemical Society*, *137*(21), 6730-6733. https://doi.org/10.1021/jacs.5b01994

Kuo, Y. (1992). Reactive ion etching of sputter deposited tantalum oxide and its etch selectivity to tantalum. *Journal of the Electrochemical Society*, *139*(2), 579. https://doi.org/10.1149/1.2069261

Liu, L., Yellinek, S., Valdinger, I., Donval, A., & Mandler, D. (2015). Important implications of the electrochemical reduction of ITO. *Electrochimica Acta*, *176*, 1374-1381. https://doi.org/10.1016/j.electacta.2015.07.129

Macher, S., Rumpel, M., Schott, M., Posset, U., Giffin, G. A., & Löbmann, P. (2020). Avoiding voltage-induced degradation in PET-ITO-based flexible electrochromic devices. *ACS applied materials & interfaces*, *12*(32), 36695-36705. https://doi.org/10.1021/acsami.0c07860

Mahmoudi, A., Faraoun, H. I., Benabadji, M. K., Abdellaoui, I., & Dergal, M. (2016). Structural, electronic and optical properties of Li intercalated on MO_3 (M: Mo, W): A first principle investigation. *Solid State Communications*, *229*, 37-42. https://doi.org/10.1016/j.ssc.2016.01.001

Minami, T. (2008). Present status of transparent conducting oxide thin-film development for Indium-Tin-Oxide (ITO) substitutes. *Thin Solid Films*, *516*(17), 5822-5828 https://doi.org/10.1016/j.tsf.2007.10.063

Monk, P., Mortimer, R., & Rosseinsky, D. *Electrochromism and electrochromic devices*. Cambridge university press, 2007.
Monk, P., Mortimer, R., & Rosseinsky, D. (2007). *Electrochromism and electrochromic devices*. Cambridge university press.

Moulder, J. F., Stickle, W. F., Sobol, P. E., Bomben, K. D., & Muilenberg, G. E. (1992). Handbook of X-ray photoelectron spectroscopy Perkin–Elmer. *Eden Prairie*.

Mullica, D. F., Beall, G. W., Milligan, W. O., Korp, J. D., & Bernal, I. (1979). The crystal structure of cubic In (OH) 3 by X-ray and neutron diffraction methods. *Journal of Inorganic and Nuclear Chemistry*, *41*(3), 277-282. https://doi.org/10.1016/0022-1902(79)80133-5

Perez, I. (2023). Ab initio methods for the computation of physical properties and performance parameters of electrochemical energy storage devices. *Physical Chemistry Chemical Physics*, *25*(3), 1476-1503. https://doi.org/10.1039/D2CP03611H

Perez, I., Faudoa, J. C. M., Acuña, J. R. A., & Galindo, J. T. E. (2021). Influence of lithium interstitial doping on the optoelectronic properties of NiO and WO3. *Computational Materials Science*, *190*, 110248. https://doi.org/10.1016/j.commatsci.2020.110248

Perez, I., Sosa, V., Gamboa, F., Elizalde Galindo, J. T., Enríquez-Carrejo, J. L., Farías, R., & Mani González, P. G. (2018). Influence of post-deposition annealing on the chemical states of crystalline tantalum pentoxide films. *Applied Physics A*, *124*(11), 792. https://doi.org/10.1007/s00339-018-2198-9

Perez, I., Sosa, V., Perera, F. G., Galindo, J. T. E., Enríquez-Carrejo, J. L., & González, P. G. M. (2019). Effect of ion bombardment on the chemical properties of crystalline tantalum pentoxide films. *Vacuum*, *165*, 274-282. https://doi.org/10.1016/j.vacuum.2019.04.037

Pollard, K. D., & Puddephatt, R. J. (1999). Chemical vapor deposition of tantalum oxide from tetraethoxo (β-diketonato) tantalum (V) complexes. *Chemistry of materials*, *11*(4), 1069-1074. https://doi.org/10.1021/cm981047a

Pramudita, J. C., Peterson, V. K., Kimpton, J. A., & Sharma, N. (2017). Potassium-ion intercalation in graphite within a potassium-ion battery examined using in situ X-ray diffraction. *Powder Diffraction*, *32*(S2), S43-S48. https://doi.org/10.1017/S0885715617000902

Ren, Y., Zhou, X., & Zhao, G. (2018). Facile preparation of FTO nanocrystalline films with excellent NIR electrochromic properties by a novel chelating solution route. *Materials Letters*, *213*, 204-207. https://doi.org/10.1016/j.matlet.2017.11.081

Shiratsuchi, R., Hongo, K., Nogami, G., & Ishimaru, S. (1992). Reduction of CO 2 on Fluorine-Doped SnO2 Thin-Film Electrodes. *Journal of the Electrochemical Society*, *139*(9), 2544. https://doi.org/10.1149/1.2221260

Smith, J. F., & Schneider, V. L. (1964). Anisotropic thermal expansion of indium. *Journal of the Less Common Metals*, *7*(1), 17-22. https://doi.org/10.1016/0022-5088(64)90013-X

Spada, E. R., De Paula, F. R., Cid, C. P., Candiotto, G., Faria, R. M., & Sartorelli, M. L. (2013). Role of acidic and basic electrolytes on the structure and morphology of cathodically reduced indium tin oxide (ITO) substrates. *Electrochimica Acta*, *108*, 520-524. https://doi.org/10.1016/j.electacta.2013.06.077

Svensson, J. S. E. M., & Granqvist, C. G. (1985). No visible electrochromism in high-quality e-beam evaporated In 2 O 3: Sn films. *Applied optics*, *24*(15), 2284-2285. https://doi.org/10.1364/AO.24.002284

Wang, D., Wei, L., Shi, P., Chen, Y., Yan, S., Tian, Y., & Jiao, J. (2019). Electrochromic behavior of fluorine-doped tin oxide film via guided motion of Li ions. *Journal of Alloys and Compounds*, *771*, 100-105. https://doi.org/10.1016/j.jallcom.2018.08.268

Wen, R. T., Granqvist, C. G., & Niklasson, G. A. (2015). Eliminating degradation and uncovering ion-trapping dynamics in electrochromic WO3 thin films. *Nature materials*, *14*(10), 996-1001. https://doi.org/10.1038/nmat4368

Wu, W., Wang, M., Ma, J., Cao, Y., & Deng, Y. (2018). Electrochromic metal oxides: recent progress and prospect. *Advanced Electronic Materials*, *4*(8), 1800185. https://doi.org/10.1002/aelm.201800185

Zhong, Q., Dahn, J. R., & Colbow, K. (1992). Lithium intercalation into WO 3 and the phase diagram of Li x WO 3. *Physical Review B*, *46*(4), 2554. https://doi.org/10.1103/PhysRevB.46.2554